Observation and Mass Measurement of the Baryon Ξ_b^-

T. Aaltonen,[23] A. Abulencia,[24] J. Adelman,[13] T. Affolder,[10] T. Akimoto,[55] M. G. Albrow,[17] S. Amerio,[43] D. Amidei,[35] A. Anastassov,[52] K. Anikeev,[17] A. Annovi,[19] J. Antos,[14] M. Aoki,[55] G. Apollinari,[17] T. Arisawa,[57] A. Artikov,[15] W. Ashmanskas,[17] A. Attal,[3] A. Aurisano,[53] F. Azfar,[42] P. Azzi-Bacchetta,[43] P. Azzurri,[46] N. Bacchetta,[43] W. Badgett,[17] A. Barbaro-Galtieri,[29] V. E. Barnes,[48] B. A. Barnett,[25] S. Baroiant,[7] V. Bartsch,[31] G. Bauer,[33] P.-H. Beauchemin,[34] F. Bedeschi,[46] S. Behari,[25] G. Bellettini,[46] J. Bellinger,[59] A. Belloni,[33] D. Benjamin,[16] A. Beretvas,[17] J. Beringer,[29] T. Berry,[30] A. Bhatti,[50] M. Binkley,[17] D. Bisello,[43] I. Bizjak,[31] R. E. Blair,[2] C. Blocker,[6] B. Blumenfeld,[25] A. Bocci,[16] A. Bodek,[49] V. Boisvert,[49] G. Bolla,[48] A. Bolshov,[33] D. Bortoletto,[48] J. Boudreau,[47] A. Boveia,[10] B. Brau,[10] L. Brigliadori,[5] C. Bromberg,[36] E. Brubaker,[13] J. Budagov,[15] H. S. Budd,[49] S. Budd,[24] K. Burkett,[17] G. Busetto,[43] P. Bussey,[21] A. Buzatu,[34] K. L. Byrum,[2] S. Cabrera,[16,q] M. Campanelli,[20] M. Campbell,[35] F. Canelli,[17] A. Canepa,[45] S. Carrillo,[18,i] D. Carlsmith,[59] R. Carosi,[46] S. Carron,[34] B. Casal,[11] M. Casarsa,[54] A. Castro,[5] P. Catastini,[46] D. Cauz,[54] M. Cavalli-Sforza,[3] A. Cerri,[29] L. Cerrito,[31,m] S. H. Chang,[28] Y. C. Chen,[1] M. Chertok,[7] G. Chiarelli,[46] G. Chlachidze,[17] F. Chlebana,[17] I. Cho,[28] K. Cho,[28] D. Chokheli,[15] J. P. Chou,[22] G. Choudalakis,[33] S. H. Chuang,[52] K. Chung,[12] W. H. Chung,[59] Y. S. Chung,[49] M. Cilijak,[46] C. I. Ciobanu,[24] M. A. Ciocci,[46] A. Clark,[20] D. Clark,[6] M. Coca,[16] G. Compostella,[43] M. E. Convery,[50] J. Conway,[7] B. Cooper,[31] K. Copic,[35] M. Cordelli,[19] G. Cortiana,[43] F. Crescioli,[46] C. Cuenca Almenar,[7,q] J. Cuevas,[11,l] R. Culbertson,[17] J. C. Cully,[35] S. DaRonco,[43] M. Datta,[17] S. D'Auria,[21] T. Davies,[21] D. Dagenhart,[17] P. de Barbaro,[49] S. De Cecco,[51] A. Deisher,[29] G. De Lentdecker,[49,c] G. De Lorenzo,[3] M. Dell'Orso,[46] F. Delli Paoli,[43] L. Demortier,[50] J. Deng,[16] M. Deninno,[5] D. De Pedis,[51] P. F. Derwent,[17] G. P. Di Giovanni,[44] C. Dionisi,[51] B. Di Ruzza,[54] J. R. Dittmann,[4] M. D'Onofrio,[3] C. Dörr,[26] S. Donati,[46] P. Dong,[8] J. Donini,[43] T. Dorigo,[43] S. Dube,[52] J. Efron,[39] R. Erbacher,[7] D. Errede,[24] S. Errede,[24] R. Eusebi,[17] H. C. Fang,[29] S. Farrington,[30] I. Fedorko,[46] W. T. Fedorko,[13] R. G. Feild,[60] M. Feindt,[26] J. P. Fernandez,[32] R. Field,[18] G. Flanagan,[48] R. Forrest,[7] S. Forrester,[7] M. Franklin,[22] J. C. Freeman,[29] I. Furic,[13] M. Gallinaro,[50] J. Galyardt,[12] J. E. Garcia,[46] F. Garberson,[10] A. F. Garfinkel,[48] C. Gay,[60] H. Gerberich,[24] D. Gerdes,[35] S. Giagu,[51] P. Giannetti,[46] K. Gibson,[47] J. L. Gimmell,[49] C. Ginsburg,[17] N. Giokaris,[15,a] M. Giordani,[54] P. Giromini,[19] M. Giunta,[46] G. Giurgiu,[25] V. Glagolev,[15] D. Glenzinski,[17] M. Gold,[37] N. Goldschmidt,[18] J. Goldstein,[42,b] A. Golossanov,[17] G. Gomez,[11] G. Gomez-Ceballos,[33] M. Goncharov,[53] O. González,[32] I. Gorelov,[37] A. T. Goshaw,[16] K. Goulianos,[50] A. Gresele,[43] S. Grinstein,[22] C. Grosso-Pilcher,[13] R. C. Group,[17] U. Grundler,[24] J. Guimaraes da Costa,[22] Z. Gunay-Unalan,[36] C. Haber,[29] K. Hahn,[33] S. R. Hahn,[17] E. Halkiadakis,[52] A. Hamilton,[20] B.-Y. Han,[49] J. Y. Han,[49] R. Handler,[59] F. Happacher,[19] K. Hara,[55] D. Hare,[52] M. Hare,[56] S. Harper,[42] R. F. Harr,[58] R. M. Harris,[17] M. Hartz,[47] K. Hatakeyama,[50] J. Hauser,[8] C. Hays,[42] M. Heck,[26] A. Heijboer,[45] B. Heinemann,[29] J. Heinrich,[45] C. Henderson,[33] M. Herndon,[59] J. Heuser,[26] D. Hidas,[16] C. S. Hill,[10,b] D. Hirschbuehl,[26] A. Hocker,[17] A. Holloway,[22] S. Hou,[1] M. Houlden,[30] S.-C. Hsu,[9] B. T. Huffman,[42] R. E. Hughes,[39] U. Husemann,[60] J. Huston,[36] J. Incandela,[10] G. Introzzi,[46] M. Iori,[51] A. Ivanov,[7] B. Iyutin,[33] E. James,[17] D. Jang,[52] B. Jayatilaka,[16] D. Jeans,[51] E. J. Jeon,[28] S. Jindariani,[18] W. Johnson,[7] M. Jones,[48] K. K. Joo,[28] S. Y. Jun,[12] J. E. Jung,[28] T. R. Junk,[24] T. Kamon,[53] P. E. Karchin,[58] Y. Kato,[41] Y. Kemp,[26] R. Kephart,[17] U. Kerzel,[26] V. Khotilovich,[53] B. Kilminster,[39] D. H. Kim,[28] H. S. Kim,[28] J. E. Kim,[28] M. J. Kim,[17] S. B. Kim,[28] S. H. Kim,[55] Y. K. Kim,[13] N. Kimura,[55] L. Kirsch,[6] S. Klimenko,[18] M. Klute,[33] B. Knuteson,[33] B. R. Ko,[16] K. Kondo,[57] D. J. Kong,[28] J. Konigsberg,[18] A. Korytov,[18] A. V. Kotwal,[16] A. C. Kraan,[45] J. Kraus,[24] M. Kreps,[26] J. Kroll,[45] N. Krumnack,[4] M. Kruse,[16] V. Krutelyov,[10] T. Kubo,[55] S. E. Kuhlmann,[2] T. Kuhr,[26] N. P. Kulkarni,[58] Y. Kusakabe,[57] S. Kwang,[13] A. T. Laasanen,[48] S. Lai,[34] S. Lami,[46] S. Lammel,[17] M. Lancaster,[31] R. L. Lander,[7] K. Lannon,[39] A. Lath,[52] G. Latino,[46] I. Lazzizzera,[43] T. LeCompte,[2] J. Lee,[49] J. Lee,[28] Y. J. Lee,[28] S. W. Lee,[53,o] R. Lefèvre,[20] N. Leonardo,[33] S. Leone,[46] S. Levy,[13] J. D. Lewis,[17] C. Lin,[60] C. S. Lin,[17] M. Lindgren,[17] E. Lipeles,[9] A. Lister,[7] D. O. Litvintsev,[17] T. Liu,[17] N. S. Lockyer,[45] A. Loginov,[60] M. Loreti,[43] R.-S. Lu,[1] D. Lucchesi,[43] P. Lujan,[29] P. Lukens,[17] G. Lungu,[18] L. Lyons,[42] J. Lys,[29] R. Lysak,[14] E. Lytken,[48] P. Mack,[26] D. MacQueen,[34] R. Madrak,[17] K. Maeshima,[17] K. Makhoul,[33] T. Maki,[23] P. Maksimovic,[25] S. Malde,[42] S. Malik,[31] G. Manca,[30] A. Manousakis,[15,a] F. Margaroli,[5] R. Marginean,[17] C. Marino,[26] C. P. Marino,[24] A. Martin,[60] M. Martin,[25] V. Martin,[21,g] M. Martínez,[3] R. Martínez-Ballarín,[32] T. Maruyama,[55] P. Mastrandrea,[51] T. Masubuchi,[55] H. Matsunaga,[55] M. E. Mattson,[58] R. Mazini,[34] P. Mazzanti,[5] K. S. McFarland,[49] P. McIntyre,[53] R. McNulty,[30,f] A. Mehta,[30] P. Mehtala,[23] S. Menzemer,[11,h] A. Menzione,[46] P. Merkel,[48] C. Mesropian,[50] A. Messina,[36] T. Miao,[17] N. Miladinovic,[6] J. Miles,[33] R. Miller,[36] C. Mills,[10] M. Milnik,[26] A. Mitra,[1] G. Mitselmakher,[18] A. Miyamoto,[27] S. Moed,[20] N. Moggi,[5] B. Mohr,[8] C. S. Moon,[28] R. Moore,[17] M. Morello,[46] P. Movilla Fernandez,[29] J. Mülmenstädt,[29] A. Mukherjee,[17] Th. Muller,[26]

R. Mumford,[25] P. Murat,[17] M. Mussini,[5] J. Nachtman,[17] A. Nagano,[55] J. Naganoma,[57] K. Nakamura,[55] I. Nakano,[40] A. Napier,[56] V. Necula,[16] C. Neu,[45] M. S. Neubauer,[9] J. Nielsen,[29,n] L. Nodulman,[2] O. Norniella,[3] E. Nurse,[31] S. H. Oh,[16] Y. D. Oh,[28] I. Oksuzian,[18] T. Okusawa,[41] R. Oldeman,[30] R. Orava,[23] K. Osterberg,[23] C. Pagliarone,[46] E. Palencia,[11] V. Papadimitriou,[17] A. Papaikonomou,[26] A. A. Paramonov,[13] B. Parks,[39] S. Pashapour,[34] J. Patrick,[17] G. Pauletta,[54] M. Paulini,[12] C. Paus,[33] D. E. Pellett,[7] A. Penzo,[54] T. J. Phillips,[16] G. Piacentino,[46] J. Piedra,[44] L. Pinera,[18] K. Pitts,[24] C. Plager,[8] L. Pondrom,[59] X. Portell,[3] O. Poukhov,[15] N. Pounder,[42] F. Prakoshyn,[15] A. Pronko,[17] J. Proudfoot,[2] F. Ptohos,[19,e] G. Punzi,[46] J. Pursley,[25] J. Rademacker,[42,b] A. Rahaman,[47] V. Ramakrishnan,[59] N. Ranjan,[48] I. Redondo,[32] B. Reisert,[17] V. Rekovic,[37] P. Renton,[42] M. Rescigno,[51] S. Richter,[26] F. Rimondi,[5] L. Ristori,[46] A. Robson,[21] T. Rodrigo,[11] E. Rogers,[24] S. Rolli,[56] R. Roser,[17] M. Rossi,[54] R. Rossin,[10] P. Roy,[34] A. Ruiz,[11] J. Russ,[12] V. Rusu,[13] H. Saarikko,[23] A. Safonov,[53] W. K. Sakumoto,[49] G. Salamanna,[51] O. Saltó,[3] L. Santi,[54] S. Sarkar,[51] L. Sartori,[46] K. Sato,[17] P. Savard,[34] A. Savoy-Navarro,[44] T. Scheidle,[26] P. Schlabach,[17] E. E. Schmidt,[17] M. P. Schmidt,[60] M. Schmitt,[38] T. Schwarz,[7] L. Scodellaro,[11] A. L. Scott,[10] A. Scribano,[46] F. Scuri,[46] A. Sedov,[48] S. Seidel,[37] Y. Seiya,[41] A. Semenov,[15] L. Sexton-Kennedy,[17] A. Sfyrla,[20] S. Z. Shalhout,[58] M. D. Shapiro,[29] T. Shears,[30] P. F. Shepard,[47] D. Sherman,[22] M. Shimojima,[55,k] M. Shochet,[13] Y. Shon,[59] I. Shreyber,[20] A. Sidoti,[46] P. Sinervo,[34] A. Sisakyan,[15] A. J. Slaughter,[17] J. Slaunwhite,[39] K. Sliwa,[56] J. R. Smith,[7] F. D. Snider,[17] R. Snihur,[34] M. Soderberg,[35] A. Soha,[7] S. Somalwar,[52] V. Sorin,[36] J. Spalding,[17] F. Spinella,[46] T. Spreitzer,[34] P. Squillacioti,[46] M. Stanitzki,[60] A. Staveris-Polykalas,[46] R. St. Denis,[21] B. Stelzer,[8] O. Stelzer-Chilton,[42] D. Stentz,[38] J. Strologas,[37] D. Stuart,[10] J. S. Suh,[28] A. Sukhanov,[18] H. Sun,[56] I. Suslov,[15] T. Suzuki,[55] A. Taffard,[24,p] R. Takashima,[40] Y. Takeuchi,[55] R. Tanaka,[40] M. Tecchio,[35] P. K. Teng,[1] K. Terashi,[50] J. Thom,[17,d] A. S. Thompson,[21] E. Thomson,[45] P. Tipton,[60] V. Tiwari,[12] S. Tkaczyk,[17] D. Toback,[53] S. Tokar,[14] K. Tollefson,[36] T. Tomura,[55] D. Tonelli,[46] S. Torre,[19] D. Torretta,[17] S. Tourneur,[44] W. Trischuk,[34] S. Tsuno,[40] Y. Tu,[45] N. Turini,[46] F. Ukegawa,[55] S. Uozumi,[55] S. Vallecorsa,[20] N. van Remortel,[23] A. Varganov,[35] E. Vataga,[37] F. Vazquez,[18,i] G. Velev,[17] C. Vellidis,[46,a] G. Veramendi,[24] V. Veszpremi,[48] M. Vidal,[32] R. Vidal,[17] I. Vila,[11] R. Vilar,[11] T. Vine,[31] M. Vogel,[37] I. Vollrath,[34] I. Volobouev,[29,o] G. Volpi,[46] F. Würthwein,[9] P. Wagner,[53] R. G. Wagner,[2] R. L. Wagner,[17] J. Wagner,[26] W. Wagner,[26] R. Wallny,[8] S. M. Wang,[1] A. Warburton,[34] D. Waters,[31] M. Weinberger,[53] W. C. Wester III,[17] B. Whitehouse,[56] D. Whiteson,[45,p] A. B. Wicklund,[2] E. Wicklund,[17] G. Williams,[34] H. H. Williams,[45] P. Wilson,[17] B. L. Winer,[39] P. Wittich,[17,d] S. Wolbers,[17] C. Wolfe,[13] T. Wright,[35] X. Wu,[20] S. M. Wynne,[30] A. Yagil,[9] K. Yamamoto,[41] J. Yamaoka,[52] T. Yamashita,[40] C. Yang,[60] U. K. Yang,[13,j] Y. C. Yang,[28] W. M. Yao,[29] G. P. Yeh,[17] J. Yoh,[17] K. Yorita,[13] T. Yoshida,[41] G. B. Yu,[49] I. Yu,[28] S. S. Yu,[17] J. C. Yun,[17] L. Zanello,[51] A. Zanetti,[54] I. Zaw,[22] X. Zhang,[24] J. Zhou,[52] and S. Zucchelli[5]

(CDF Collaboration)

[1]*Institute of Physics, Academia Sinica, Taipei, Taiwan 11529, Republic of China*
[2]*Argonne National Laboratory, Argonne, Illinois 60439, USA*
[3]*Institut de Fisica d'Altes Energies, Universitat Autonoma de Barcelona, E-08193, Bellaterra (Barcelona), Spain*
[4]*Baylor University, Waco, Texas 76798, USA*
[5]*Istituto Nazionale di Fisica Nucleare, University of Bologna, I-40127 Bologna, Italy*
[6]*Brandeis University, Waltham, Massachusetts 02254, USA*
[7]*University of California, Davis, Davis, California 95616, USA*
[8]*University of California, Los Angeles, Los Angeles, California 90024, USA*
[9]*University of California, San Diego, La Jolla, California 92093, USA*
[10]*University of California, Santa Barbara, Santa Barbara, California 93106, USA*
[11]*Instituto de Fisica de Cantabria, CSIC-University of Cantabria, 39005 Santander, Spain*
[12]*Carnegie Mellon University, Pittsburgh, Pennsylvania 15213, USA*
[13]*Enrico Fermi Institute, University of Chicago, Chicago, Illinois 60637, USA*
[14]*Comenius University, 842 48 Bratislava, Slovakia; Institute of Experimental Physics, 040 01 Kosice, Slovakia*
[15]*Joint Institute for Nuclear Research, RU-141980 Dubna, Russia*
[16]*Duke University, Durham, North Carolina 27708*
[17]*Fermi National Accelerator Laboratory, Batavia, Illinois 60510, USA*
[18]*University of Florida, Gainesville, Florida 32611, USA*
[19]*Laboratori Nazionali di Frascati, Istituto Nazionale di Fisica Nucleare, I-00044 Frascati, Italy*
[20]*University of Geneva, CH-1211 Geneva 4, Switzerland*
[21]*Glasgow University, Glasgow G12 8QQ, United Kingdom*
[22]*Harvard University, Cambridge, Massachusetts 02138, USA*

[23]Division of High Energy Physics, Department of Physics, University of Helsinki and Helsinki Institute of Physics, FIN-00014, Helsinki, Finland
[24]University of Illinois, Urbana, Illinois 61801, USA
[25]The Johns Hopkins University, Baltimore, Maryland 21218, USA
[26]Institut für Experimentelle Kernphysik, Universität Karlsruhe, 76128 Karlsruhe, Germany
[27]High Energy Accelerator Research Organization (KEK), Tsukuba, Ibaraki 305, Japan
[28]Center for High Energy Physics: Kyungpook National University, Taegu 702-701, Korea; Seoul National University, Seoul 151-742, Korea; SungKyunKwan University, Suwon 440-746, Korea
[29]Ernest Orlando Lawrence Berkeley National Laboratory, Berkeley, California 94720, USA
[30]University of Liverpool, Liverpool L69 7ZE, United Kingdom
[31]University College London, London WC1E 6BT, United Kingdom
[32]Centro de Investigaciones Energeticas Medioambientales y Tecnologicas, E-28040 Madrid, Spain
[33]Massachusetts Institute of Technology, Cambridge, Massachusetts 02139, USA
[34]Institute of Particle Physics: McGill University, Montréal, Canada H3A 2T8; and University of Toronto, Toronto, Canada M5S 1A7
[35]University of Michigan, Ann Arbor, Michigan 48109, USA
[36]Michigan State University, East Lansing, Michigan 48824, USA
[37]University of New Mexico, Albuquerque, New Mexico 87131, USA
[38]Northwestern University, Evanston, Illinois 60208, USA
[39]The Ohio State University, Columbus, Ohio 43210, USA
[40]Okayama University, Okayama 700-8530, Japan
[41]Osaka City University, Osaka 588, Japan
[42]University of Oxford, Oxford OX1 3RH, United Kingdom
[43]University of Padova, Istituto Nazionale di Fisica Nucleare, Sezione di Padova-Trento, I-35131 Padova, Italy
[44]LPNHE, Universite Pierre et Marie Curie/IN2P3-CNRS, UMR7585, Paris, F-75252 France
[45]University of Pennsylvania, Philadelphia, Pennsylvania 19104, USA
[46]Istituto Nazionale di Fisica Nucleare Pisa, Universities of Pisa, Siena and Scuola Normale Superiore, I-56127 Pisa, Italy
[47]University of Pittsburgh, Pittsburgh, Pennsylvania 15260, USA
[48]Purdue University, West Lafayette, Indiana 47907, USA
[49]University of Rochester, Rochester, New York 14627, USA
[50]The Rockefeller University, New York, New York 10021, USA
[51]Istituto Nazionale di Fisica Nucleare, Sezione di Roma 1, University of Rome "La Sapienza," I-00185 Roma, Italy
[52]Rutgers University, Piscataway, New Jersey 08855, USA
[53]Texas A&M University, College Station, Texas 77843, USA
[54]Istituto Nazionale di Fisica Nucleare, University of Trieste/ Udine, Italy
[55]University of Tsukuba, Tsukuba, Ibaraki 305, Japan
[56]Tufts University, Medford, Massachusetts 02155, USA
[57]Waseda University, Tokyo 169, Japan
[58]Wayne State University, Detroit, Michigan 48201, USA
[59]University of Wisconsin, Madison, Wisconsin 53706, USA
[60]Yale University, New Haven, Connecticut 06520, USA
(Received 4 July 2007; published 3 August 2007)

We report the observation and measurement of the mass of the bottom, strange baryon Ξ_b^- through the decay chain $\Xi_b^- \to J/\psi \Xi^-$, where $J/\psi \to \mu^+\mu^-$, $\Xi^- \to \Lambda\pi^-$, and $\Lambda \to p\pi^-$. A signal is observed whose probability of arising from a background fluctuation is 6.6×10^{-15}, or 7.7 Gaussian standard deviations. The Ξ_b^- mass is measured to be $5792.9 \pm 2.5(\text{stat}) \pm 1.7(\text{syst})\ \text{MeV}/c^2$.

DOI: 10.1103/PhysRevLett.99.052002 PACS numbers: 14.20.Mr, 13.30.Eg, 13.60.Rj

Since its inception, the quark model has had great success in describing the spectroscopy of hadrons. The quark model has been successful for the B mesons, where all of the ground states have been observed [1]. The spectroscopy of c baryons also agrees well with the quark model, and a rich spectrum of baryons containing b quarks is predicted [2]. However, direct observation of b baryons has been limited to a single state, the Λ_b (quark content udb) [1], until recently. Evidence for b baryons that also contain a strange quark was shown from LEP [3] through partial reconstruction of decays containing electrons and muons. Recent results from the Tevatron on the Σ_b states (quark content uub, ddb) [4] and Ξ_b^- (quark content dsb) [5] are beginning to subject the b baryons to closer examination.

In this Letter, we report the observation of a heavy baryon and measurement of its mass. The decay properties of this state are consistent with the weak decay of a b baryon, and we interpret our result as the observation of the Ξ_b^- baryon. This observation is made in $p\bar{p}$ collisions at a center of mass energy of 1.96 TeV using the Collider Detector at Fermilab (CDF II), through the decay chain $\Xi_b^- \to J/\psi \Xi^-$, where $J/\psi \to \mu^+\mu^-$, $\Xi^- \to \Lambda\pi^-$, and $\Lambda \to p\pi^-$. Charge conjugate modes are included implicitly. This measurement is based on a data sample with an integrated luminosity of 1.9 fb^{-1}.

The CDF II detector has been described in detail elsewhere [6]. This analysis primarily relies upon the tracking and muon identification systems. The tracking system consists of a silicon microstrip detector and an open-cell drift chamber (COT) that operate inside a solenoid with a 1.4 T magnetic field. Muon candidates from the decay $J/\psi \to \mu^+\mu^-$ are identified by two sets of drift chambers located radially outside the electromagnetic and hadronic calorimeters. The central muon chambers cover the pseudorapidity region $|\eta| < 0.6$ [7], and are sensitive to muons with transverse momentum $p_T > 1.4$ GeV/c. A second muon system covers the region $0.6 < |\eta| < 1.0$ and detects muons having $p_T > 2.0$ GeV/c. Muon triggering and identification are based on matching tracks measured in the muon system to COT tracks.

The analysis of the data begins with a selection of well-measured $J/\psi \to \mu^+\mu^-$ candidates. The trigger requirements are confirmed by selecting events that contain two oppositely charged muon candidates, each with matching COT and muon chamber tracks. We also require that both muon tracks have associated measurements in at least three layers of the silicon detector and a two-track invariant mass within 80 MeV/c^2 of the world-average J/ψ mass [1]. This data sample provides approximately 15×10^6 events containing J/ψ candidates, measured with an average mass resolution of 20 MeV/c^2.

The reconstruction of Ξ^- candidates uses all additional tracks found in each selected J/ψ event. Pairs of oppositely charged tracks are used to identify Λ decay candidates. The proton (pion) mass is assigned to the track with the higher (lower) momentum. This mass assignment is always correct for $\Lambda \to p\pi^-$ candidates used in this analysis because of the kinematics of Λ decay and the lower limit of ≈ 200 MeV/c in the transverse momentum acceptance of the tracking system. The Λ mass is measured with a resolution of 2.5 MeV/c^2. All intersecting pairs of tracks with an invariant mass within 10 MeV/c^2 of the world average Λ mass [1] have their track parameters recalculated according to a fit where the momenta of the two tracks are constrained to the Λ mass. The decay vertex is used to calculate the Λ displacement from the beam line in the direction of the track pair's transverse momentum. The background due to tracks originating from the primary vertex is reduced by requiring this displacement to exceed 1.0 cm. For candidates that satisfy these requirements, the remaining tracks are assigned the pion mass, and $\Lambda\pi^-$ combinations are identified that are consistent with the decay process $\Xi^- \to \Lambda\pi^-$. In order to obtain the best possible $\Lambda\pi^-$ mass resolution, the reconstruction uses a fit on the three tracks that simultaneously constrains the Λ decay products to the Λ mass, and the Λ trajectory to intersect with the helix of the Ξ^- decay pion. For all Ξ^- candidates, the reconstructed decay position of the Λ candidate is required to be radially displaced at least 1.0 cm with respect to the reconstructed decay vertex of the Ξ^- candidate.

The majority of Ξ^- candidates have $p_T > 1.5$ GeV/c. This, along with the long lifetime of the Ξ^- ($c\tau = 4.9$ cm) [1], results in a significant fraction of the Ξ^- candidates having decay vertices located several centimeters radially outward from the beam line. Therefore, we are able to refine the Ξ^- reconstruction by making use of the improved determination of the trajectory that can be obtained by tracking the Ξ^- in the silicon detector. The Ξ^- candidates have an additional fit performed on the three tracks that simultaneously constrains both the Λ and Ξ^- masses of the appropriate track combinations, and provides the best possible estimate of the Ξ^- momentum and decay position. The result of this fit is used to define a helix that serves as the seed for an algorithm that searches for silicon detector hits associated with the Ξ^- track. We retain for further analysis all Ξ^- candidates with measurements in at least two layers of the silicon detector. This technique provides excellent impact parameter resolution for the Ξ^- track (average of 60 μm), and has been used previously [8]. The $\Lambda\pi^-$ invariant mass spectrum of all combinations that satisfy these requirements is shown in Fig. 1. Approximately 23 500 Ξ^- candidates above the combinatorial background are identified. The Ξ_b^- search includes the subset of these combinations with an invariant mass within 10 MeV/c^2 of the world average Ξ^- mass [1].

The mass resolution for the $J/\psi\Xi^-$ final state is studied with a Monte Carlo simulation that generates b quarks

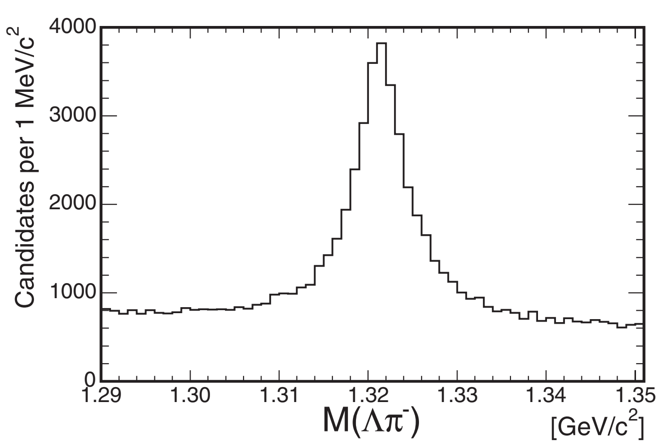

FIG. 1. The invariant mass distribution of $\Lambda\pi^-$ combinations having an associated track in the silicon detector in events containing J/ψ candidates.

according to a next-to-leading-order calculation [9], and produces Ξ_b^- events by simulating b quark fragmentation [10]. The decay $\Xi_b^- \to J/\psi \Xi^-$ is simulated with EVTGEN [11]. The generated events are used as input to the detector and trigger simulations based on a GEANT3 description [12] and processed through the same reconstruction and analysis algorithms used for the data. Analysis of the simulated Ξ_b^- events shows that a 10% improvement in mass resolution can be obtained if the momenta of the Ξ^- decay products are allowed to vary in the fit of the Ξ_b^- candidate, rather than simply using the Ξ^- track. Consequently, a procedure that simultaneously fits the five tracks of the final state, constrains the three vertices of the decay chain to the appropriate topology, and constrains the masses of the J/ψ, Ξ^-, and Λ to their world-average masses, is used to provide the best estimate of the $J/\psi \Xi^-$ mass. The average Ξ_b^- mass resolution obtained from simulated events is found to be approximately 15 MeV$/c^2$. In particular, we note that the $J/\psi \Xi^-$ invariant mass resolution is comparable to the mass resolution obtained with the CDF II detector for other B hadrons with a J/ψ in the final state [13].

The selection used to isolate the $\Xi_b^- \to J/\psi \Xi^-$ decay process is guided by the properties of other B hadrons that include a J/ψ in the final state. The important ones include the lifetime of the ground-state B hadrons and the energy available in the decay. The $B^\pm$, B^0, and B_s mesons and Λ_b baryon, all appear to have lifetimes dominated by the weak decay of the b quark. We expect the same to hold true for the Ξ_b^- and for its lifetime to be comparable to these states. In addition, these particles all decay to final states $J/\psi X$, where X is a single hadron. In these decays the momentum carried by the decay products in the rest frame of the B hadron falls in the fairly narrow range of 1570–1744 MeV$/c^2$ for decays where only the lightest decay products are considered. We expect the energy released in the decay of the Ξ_b^- to be comparable. This expectation is also consistent with the range of theoretical predictions (5788–5812 MeV$/c^2$) for the Ξ_b^- mass [2]. Consequently, we have chosen a Ξ_b^- search strategy that will provide an optimal sensitivity for a final state that shares similar properties with these well-established B hadrons.

We have developed the event selection by studying $B^\pm \to J/\psi K^\pm$ decays. This final state is identified by assigning the $K^\pm$ mass to all tracks not used in the J/ψ reconstruction. Each three-track combination must satisfy a fit where the tracks are required to originate from a common vertex and the invariant mass of the muon pair is constrained to the world-average J/ψ mass [1]. Approximately 30 000 $B^\pm$ candidates are identified in this sample. Several characteristics of the final state are used as selection requirements to obtain a $B^\pm$ signal with very little background. Minimum transverse momentum requirements on the $K^\pm$ and $B^\pm$ candidates are used to suppress backgrounds from the event that are not related to the $B^\pm$ decay. The trajectory of the $K^\pm$ is required to originate from the $B^\pm$ decay vertex by placing a requirement on its impact parameter $d_{SV}(K)$ and associated uncertainty $\sigma_{d_{SV}}(K)$ with respect to the vertex found in the J/ψ fit. Similar impact parameter quantities $d_{PV}(K)$ and $\sigma_{d_{PV}}(K)$ measured with respect to the primary vertex are used to remove tracks that originate from the prompt background. Reasonable vertex quality is assured by placing a minimum value on the accepted probability $P(\chi^2)$ of the mass- and vertex-constrained fit used to obtain the $B^\pm$ candidate. We suppress the promptly produced combinatorial background by rejecting candidates with low proper decay time, $t \equiv \vec{L}_T \cdot \vec{p}_T(B) \frac{M(B)}{|p_T(B)|^2}$, where $M(B)$ is the mass of the $B^\pm$ candidate, $\vec{p}_T(B)$ is the transverse momentum of the $B^\pm$ candidate, and $\vec{L}_T$ is the transverse displacement of the $B^\pm$ decay vertex from the beam line. A requirement on proper decay time uncertainty σ_t removes poorly-reconstructed combinations. We also reject combinations that are inconsistent with having originated from the beam line by requiring a small magnitude of the impact of the $B^\pm$ candidate, $\vec{d}_{PV}(B) \equiv \vec{L}_T \times \vec{p}_T(B)/|p_T(B)|$, and a small angle β between $\vec{L}_T$ and $\vec{p}_T(B)$.

This analysis uses a two-step selection procedure. Final selection criteria are listed in Table I. We first impose the "standard" selection requirements listed there and retain all $J/\psi K^\pm$ combinations that satisfy them. Any combination that fails only one of the standard selection requirements is also allowed into the final sample if it satisfies both of the p_T requirements of the "high-p_T" selection requirements and fails no more than one of the other requirements in this set. The combination of standard and "high-p_T" requirements reduce the background in the $B^\pm \to J/\psi K^\pm$ sample to approximately 400 combinations, while retaining a signal of 16 000 $B^\pm$ candidates.

As is done for the reconstruction of the $B^\pm$, the treatment of the $J/\psi \Xi^-$ candidates requires a mass- and vertex-

TABLE I. Selection variables and requirements for the standard selection and "high-p_T" selection as described in the text. Here "K" refers to the third track combined with the J/ψ and is a $K^\pm$ or Ξ^- candidate for the $B^\pm$ or Ξ_b^- candidates, respectively. Similarly, "B" refers to either $B^\pm$ or Ξ_b^-, as is appropriate.

Selection variable	Standard	High-p_T
$p_T(K)$	>1.7 GeV$/c$	>2.5 GeV$/c$
$p_T(B)$	>5 GeV$/c$	>6 GeV$/c$
$\lvert d_{SV}(K)\rvert$	<100 μm	<80 μm
$\lvert d_{PV}(K)\rvert/\sigma_{d_{PV}(K)}$	>2.5	>3
$P(\chi^2)$	>0.1%	>1%
$\lvert d_{PV}(B)\rvert$	<75 μm	<60 μm
ct	>80 μmm	>100 μm
$c\sigma_t$	<30 μm	<25 μm
β	<0.4 rad	<0.3 rad

constrained fit on the muon candidates and the Ξ^- track. The selection criteria in Table I are applied to the $J/\psi\Xi^-$ sample where we simply exchange K^- for Ξ^- and $B^\pm$ for Ξ_b^- where appropriate. Combinations that satisfy these requirements form the final set of Ξ_b^- candidates. The invariant mass of each candidate is obtained with the full five-track fit, and the resulting $J/\psi\Xi^-$ mass distribution is shown in Fig. 2.

The mass resolution estimate for the Ξ_b^- implies that more than 95% of a Ξ_b^- signal will occupy an invariant mass bin with a width of 75 MeV$/c^2$. The data shown in Fig. 2 contain 18 candidates in the 75 MeV$/c^2$ range of 5750–5825 MeV$/c^2$. We model the combinatorial background by considering candidates in the range 5700–6500 MeV$/c^2$; the data yield 23 candidates in this range. No events contribute multiple candidates. The upper limit of this range is chosen arbitrarily, and has no impact on the result. The lower limit is chosen to avoid partially reconstructed $\Xi_b^{-,0} \to J/\psi\Xi^- X$ decays, where X represents additional undetected particles. We assume that the mass distribution of the combinatorial background is uniform and that the occupancy due to background combinations in any particular 75 MeV$/c^2$ mass bin within the 800 MeV$/c^2$ search range can be described by a binomial distribution, with a single event probability given by the ratio of the two mass ranges used. The probability that the number of candidates observed in the 5750–5825 MeV$/c^2$ mass range is due to a background fluctuation is estimated as the binomial probability of 18 or more events from a sample of 23 total occurrences and a single event probability of 75/800. This probability is 6.6×10^{-15}, equivalent to a 7.7σ variation from a Gaussian distribution. Consequently, we interpret the data distribution shown in Fig. 2 to be the observation of a resonance, with a width consistent with the detector resolution. Comparable distributions of $J/\psi\Lambda\pi^+$ and $J/\psi\Lambda\pi^-$, where the $\Lambda\pi^-$ does not form a Ξ^-, yield no significant enhancement at any mass within the range of this analysis.

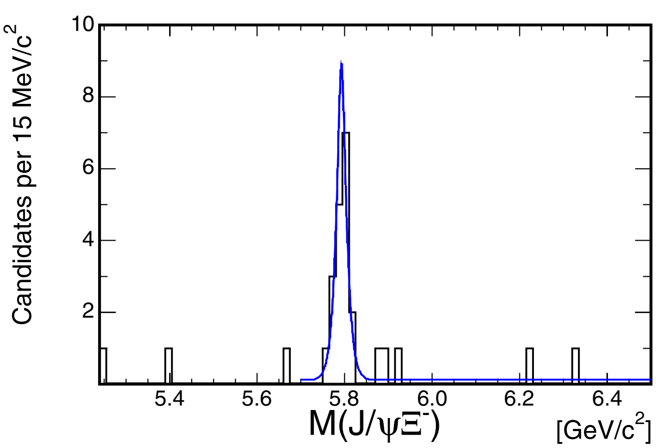

FIG. 2 (color online). The $J/\psi\Xi^-$ invariant mass distribution for combinations that satisfy the selection requirements. The projection of the fit function is overlaid on the data.

The masses and their uncertainties obtained from the five-track final state fit method are used in an unbinned likelihood fit to measure the Ξ_b^- mass. The negative log-likelihood function that is minimized has the form

$$\mathcal{L} = -2\sum_{i=1}^{N} \ln[fG(m_i, m_0, s_m\sigma_i^m) + (1-f)\mathcal{C}], \qquad (1)$$

where m_i is the mass obtained for a single candidate, σ_i^m is the uncertainty on that mass as estimated from the track parameters for the candidate, $G(m_i, m_0, s_m\sigma_i^m)$ is a Gaussian distribution with average m_0 and characteristic width $s_m\sigma_i^m$, and $\mathcal{C}$ is a constant background term. The quantities obtained from the fitting procedure include f, the fraction of the events found in the signal, m_0, the best average mass, and s_m, a scale factor on the mass uncertainty which accounts for a possible shift in the mass uncertainty. This procedure yields a best estimate for the Ξ_b^- mass of 5792.9 ± 2.5 MeV$/c^2$. The uncertainty scale factor is determined to be 2.0 ± 0.4, which is consistent with the value of 1.6 ± 0.2 obtained with simulated Ξ_b^- candidates. The signal fraction is calculated to be 0.76 ± 0.09, giving a yield of 17.5 ± 4.3 Ξ_b^- candidates in this data sample. The projection of the fit function is superimposed on Fig. 2.

Several systematic effects have been considered for their impact on the Ξ_b^- mass measurement. The overall momentum scale of the tracking system is established by calibrating with the well-measured J/ψ, $\psi(2S)$, and Υ states [13]. The momentum scale uncertainty contributes a systematic uncertainty of ± 0.4 MeV$/c^2$ on the Ξ_b^- mass measurement. Alignment and material distribution of the tracking system contributes an additional ± 0.6 MeV$/c^2$ of uncertainty. The method requires knowledge of the mass of the final state Ξ^-, a quantity that is known to ± 0.13 MeV$/c^2$ [1]. The mass uncertainty of the J/ψ is included in the momentum scale calibration, and the mass uncertainty of the Λ (± 0.006 MeV$/c^2$) is negligible for this analysis. Finally, the largest systematic variation seen on the mass measurement occurs when alternative fitting models are used for the mass calculation. The signal distribution has been fit with a single Gaussian where its parameters are allowed to vary in the fit. A double Gaussian is also used, where the widths are fixed to values obtained in simulation, and only the average mass is allowed to vary. These different models for the probability distribution function of the signal create variations of ± 1.5 MeV$/c^2$ on the mass result. The individual systematic uncertainties are combined in quadrature to obtain an overall systematic uncertainty of ± 1.7 MeV$/c^2$ on the Ξ_b^- mass measurement.

In conclusion, we use the CDF II detector at the Tevatron to observe the Ξ_b^- in $p\bar{p}$ collisions. A signal with 17.5 ± 4.3 Ξ_b^- candidates and a significance of 7.7σ is seen in the decay channel $\Xi_b^- \to J/\psi\Xi^-$. The mass of this baryon is measured to be $5792.9 \pm 2.5(\text{stat}) \pm 1.7(\text{syst})\ \text{MeV}/c^2$, which is consistent with theoretical expectations [2]. The mass measurement presented is also consistent with the only other direct observation of this state [5], and represents a significant improvement in precision.

We thank the Fermilab staff and the technical staffs of the participating institutions for their vital contributions. This work was supported by the U. S. Department of Energy and National Science Foundation; the Italian Istituto Nazionale di Fisica Nucleare; the Ministry of Education, Culture, Sports, Science and Technology of Japan; the Natural Sciences and Engineering Research Council of Canada; the National Science Council of the Republic of China; the Swiss National Science Foundation; the A. P. Sloan Foundation; the Bundesministerium für Bildung und Forschung, Germany; the Korean Science and Engineering Foundation and the Korean Research Foundation; the Science and Technology Facilities Council and the Royal Society, UK; the Institut National de Physique Nucleaire et Physique des Particules/CNRS; the Russian Foundation for Basic Research; the Comisión Interministerial de Ciencia y Tecnología, Spain; the European Community's Human Potential Programme; the Slovak R&D Agency; and the Academy of Finland.

[a]Visiting scientist from University of Athens, 15784 Athens, Greece.

[b]Visiting scientist from University of Bristol, Bristol BS8 1TL, United Kingdom.

[c]Visiting scientist from University Libre de Bruxelles, B-1050 Brussels, Belgium.

[d]Visiting scientist from Cornell University, Ithaca, NY 14853, USA.

[e]Visiting scientist from University of Cyprus, Nicosia CY-1678, Cyprus.

[f]Visiting scientist from University College Dublin, Dublin 4, Ireland.

[g]Visiting scientist from University of Edinburgh, Edinburgh EH9 3JZ, United Kingdom.

[h]Visiting scientist from University of Heidelberg, D-69120 Heidelberg, Germany.

[i]Visiting scientist from Universidad Iberoamericana, Mexico D.F., Mexico.

[j]Visiting scientist from University of Manchester, Manchester M13 9PL, United Kingdom.

[k]Visiting scientist from Nagasaki Institute of Applied Science, Nagasaki, Japan.

[l]Visiting scientist from University de Oviedo, E-33007 Oviedo, Spain.

[m]Visiting scientist from University of London, Queen Mary College, London, E1 4NS, United Kingdom.

[n]Visiting scientist from University of California Santa Cruz, Santa Cruz, CA 95064, USA.

[o]Visiting scientist from Texas Tech University, Lubbock, TX 79409, USA.

[p]Visiting scientist from University of California, Irvine, Irvine, CA 92697, USA.

[q]Visiting scientist from IFIC(CSIC-Universitat de Valencia), 46071 Valencia, Spain.

[1] W.-M. Yao *et al.* (Particle Data Group), J. Phys. G **33**, 1 (2006).

[2] E. Jenkins, Phys. Rev. D **54**, 4515 (1996); **55**, R10 (1997); N. Mathur, R. Lewis, and R. M. Woloshyn, *ibid.* **66**, 014502 (2002); D. Ebert, R. N. Faustov and V. O. Galkin, *ibid.* **72**, 034026 (2005); M. Karliner, B. Keren-Zur, H. J. Lipkin, and J. L. Rosner, arXiv:0706.2163v5.

[3] D. Buskulic *et al.* (ALEPH Collaboration), Phys. Lett. B **384**, 449 (1996); P. Abreu *et al.* (DELPHI Collaboration), Z. Phys. C **68**, 541 (1995).

[4] T. Aaltonen *et al.* (CDF Collaboration), arXiv:0706.3868

[5] V. M. Abazov *et al.* (D0 Collaboration), Phys. Rev. Lett. **99**, 052001 (2007).

[6] D. Acosta *et al.* (CDF Collaboration), Phys. Rev. D **71**, 032001 (2005); D. Amidei *et al.*, Nucl. Instrum. Methods **350**, 73 (1994); F. Abe *et al.* (CDF Collaboration), Phys. Rev. D **50**, 2966 (1994).

[7] The pseudorapidity η is defined as $\eta \equiv -\ln[\tan(\theta/2)]$, where θ is the angle between the particle momentum and the proton beam direction. The transverse momentum p_T is defined as the component of the particle momentum perpendicular to the proton beam direction.

[8] A. Abulencia *et al.* (CDF Collaboration), Phys. Rev. D **75**, 032003 (2007).

[9] P. Nason, S. Dawson, and R. K. Ellis, Nucl. Phys. **B303**, 607 (1988); **B327**, 49 (1989).

[10] C. Peterson, D. Schlatter, I. Schmitt, and P. M. Zerwas, Phys. Rev. D **27**, 105 (1983).

[11] D. J. Lange, Nucl. Instrum. Methods Phys. Res., Sect. A **462**, 152 (2001).

[12] R. Brun, R. Hagelberg, M. Hansroul, and J.C. Lassalle, CERN Reports No. CERN-DD-78-2-REV and No. CERN-DD-78-2.

[13] D. Acosta *et al.* (CDF Collaboration), Phys. Rev. Lett. **96**, 202001 (2006).